Mechanical Flexibility and Electrical Reliability of ZnO-Al Thin Films on Polymer Substrates Under Different External Deformation

Mohammed, Dilveen W.

DOI:
10.2478/adms-2024-0003

Document Version
Publisher's PDF, also known as Version of record

Citation for published version (Harvard):
Mohammed, DW 2024, 'Mechanical Flexibility and Electrical Reliability of ZnO-Al Thin Films on Polymer Substrates Under Different External Deformation', *Advances in Materials Science*, vol. 24, no. 1, pp. 32-45. https://doi.org/10.2478/adms-2024-0003

ADVANCES IN MATERIALS SCIENCE, Vol. 24, No. 1 (79), March 2024

DOI: 10.2478/adms-2024-0003

Dilveen W. Mohammed[1,2*]

1 University of Duhok, Department of Physics, Zakho way, Duhok, Iraq
2 University of Birmingham, School of Metallurgy and Materials, Edgbaston, Birmingham, B15 2TT, United Kingdom

** dilveen@uod.ac, dilveenmohammed83@gmail.com*

MECHANICAL FLEXIBILITY AND ELECTRICAL RELIABILITY OF ZnO-Al THIN FILMS ON POLYMER SUBSTRATES UNDER DIFFERENT EXTERNAL DEFORMATION

ABSTRACT

Aluminum-doped zinc oxide (AZO) films have emerged as promising transparent electrodes for various optoelectronic applications due to their superior transparency, electrical conductivity, and cost-effectiveness compared to indium tin oxide (ITO). Despite their widespread use, investigations into the electromechanical properties of AZO films, especially under various mechanical deformations, remain limited. This study employs RF magnetron sputtering to deposit AZO films on polyethylene naphthalate (PEN) substrates and explores their mechanical behavior through uniaxial tensile fragmentation and bending tests, coupled with in-situ optical microscopy. Changes in electrical resistance of AZO films were monitored in situ during deformation. Fatigue behavior was examined to further understand mechanical failure, and SEM was used for surface characterization. A critical strain of about 3.1 percent was detected during uniaxial tensile testing, marking the onset of cracks in AZO-coated PEN. In contrast to thicker films, thinner films demonstrated improved stretchability beyond the initiation of crack onset strain. Tension and compression bending tests revealed that the material has excellent bendability, as shown by its critical radii of 5.4 mm and 3.9 mm, respectively. The bending reliability of AZO films under compression was found to be superior than that under tension.
Bending fatigue experiments demonstrated that AZO films could withstand cyclic stress without experiencing no ticeable cracks after 100 cycles and with very minor resistance change. This study contributes to the creation of more reliable and optimized flexible optoelectronic devices by giving substantial quantitative data on the performance of AZO films when exposed to mechanical stress.

Keywords: polymer substrates; ZnO:Al, PEN; bending, flexible optoelectronic devices; mechanical properties

INTRODUCTION

Device performances are strongly dependent on the optical, electrical, and mechanical characteristics of the flexible transparent conducting oxide FTCO electrodes, FTCO with superior flexibility have recently attracted a lot of attention as key components in flexible displays, organic light-emitting diodes, touch panels and solar cells. Due to their excellent

conductivity and transparency in the visible spectral range, indium tin oxide (ITO) electrodes are commonly used as FTCO materials in flexible optoelectronic devices [1].

However, indium's toxicity and high cost as a result of its scarcity mean that indium-free materials, such as other oxide film, metal thin films, graphene, metal nanowires and carbon nanotubes, have recently gained great attention as a possible replacement material to ITO [2]. Impurity-doped ZnO, like Al doped (AZO), stands out among these options due to its ideal optoelectronic performance [3], inexpensive material costs, moderate deposition temperature, and non-toxicity [4].

Various techniques including radio frequency (RF) magnetron sputtering, direct current (DC) magnetron sputtering, pulsed laser deposition, electron beam evaporation, and the sol–gel process have been utilized to fabricate AZO thin films [5].Wu and Lu reported that AZO prepared by using a sol-gel route and RF magnetron sputtering had a low electrical resistivity of 21.5 Ω cm and an optical transmittance of 85–90% in the 400–900 nm wavelength range [6]. Fernández [7] et al. also reported that AZO on polyethylene terephthalate possess good electrical and optical properties even when the substrate temperature of the deposition is lower than the optimum one.

Impurity-doped ZnO electrodes must withstand mechanical deformation during roll-to-roll manufacture or operation of flexible electronic devices. Due to mechanical mismatches between flexible organic substrate and the inorganic ceramic film, these external forces may enhance film cracking and delamination in the transparent anode layer of many optoelectronic devices. Thus mechanical failure such us crack initiation and propagation, of brittle thin film need to characterize and understand mechanical failure under different deformation such as stretching, bending, bending-fatigue or twisting, to enable optimization of design and manufacturing for flexible optoelectronic devices [4].

Various authors have reported mechanical properties of thin films on a flexible substrate using various techniques. Sierros et al. [8] studied the electromechanical behavior of carbon nanotube (CNT) film under uniaxial tension. It was pointed out that change in electrical resistance of film start at strain 25 % which is 10 times higher than that observed in the ITO coated PET. Hamasha et al. [9], used both cracks development method and electrical resistance change method to analyze the behavior of magnetron sputtered ITO thin film on PET substrate under tensile strain. They observed two types of cracks: the first type of cracks initiated at strain 4 % and propagated perpendicular to stretching direction. Second type pf cracks were denoted as lateral cracks. The direction of cracks propagation was perpendicular to the original cracks. Furthermore, Lim et al. [10] investigated the degradation and fracture of ITO coated compliant substrates under various bending conditions. They concluded that the mechanical and electrical stability of the ITO film depend on the physical property of base polymer substrate.

There is limited previous research on the mechanical durability of AZO thin film, deposited on polyester substrates. Ni et al. [11] evaluated the fracture behaviour of RF magnetron sputtered AZO films on PET substrate by using a simple bending method. They found that after a certain amount of strain is applied, both the crack density and the crack spacing of the AZO films become saturated in the tension and compression bending mode. They reported that when the film flexed in tension mode, the AZO film exhibits a larger saturation crack density compared to when the film in compression mode.

Moreover, Peng et al.[12] conducted cyclic bending fatigue experiments on AZO coated Kapton substrate and found that the percentage change in electrical resistance was significantly affected by the number of bending cycles and bending diameter. They also observed that after 1000 bending cycles, the average transmittance decreases by 3.4%.

In this work, we choose a polyethylene naphthalate (PEN) as a substrate which are most widely used in flexible electron device application. The mechanical flexibility of AZO films with various thickness prepared by RF sputtering was investigated utilizing different mechanical teste, including the in-situ uniaxial tensile and bending test. We have also focused on bending fatigue behavior of film because flexible electronic devices are susceptible to repeated bending loading during roll-to roll manufacturing or usage.

This work will improve the yield of the roll-to-roll manufacturing process, resulting in devices that are not only flexible but also reliable and robust.

EXPERIMENTAL

In this study, RF magnetron sputtering was utilized to coat heat stabilized and biaxially-oriented polymer substrates with AZO thin films of 75 nm and 200 nm thickness. The polymer substrates used were dog-bone shaped, measuring 50 mm in length, with a gauge length of 18 mm and a gauge width of 4 mm. Moore Hydraulic Press was used to cut substrates from A4 sheets of PEN Teonex 0.125mm (manufactured by DuPont Teijin Films, UK). Before being introduced into the sputtering chamber, the polymer substrates underwent a thorough cleaning process. They were first subjected to ultrasonic cleaning in acetone, followed by ethanol, and finally in deionized water, with each step lasting 5 minutes.

The deposition process took place in an argon atmosphere without introducing oxygen, and without heating the substrate or post-annealing treatment. A 4-inch diameter ceramic target AZO (2 wt% Al_2O_3-doped ZnO), positioned 20 cm away from the substrate, was used. The base pressure inside the chamber was maintained at 5.1×10^{-6} Pa. The deposition process employed a constant RF power of 55 W, a power density of 0.7 W/cm^2, a deposition pressure of 0.5 Pa, an argon flow rate of 50 sccm (standard cubic centimeter per minute at STP conditions), and a deposition rate of approximately 3.3 nm/min. A pre-sputtering treatment was conducted to effectively clean the target surface using argon plasma for a duration of 5 minutes.

The average transmittance in the visible region was measured using a Jenway 6310 spectrophotometer and found to be around 81% for the film with a thickness of 75 nm and 78 % for the film with a thickness of 200 nm. Additionally, the resistivity of the 75 and 200 nm film was determined to be 1.3×10^{-1} and 3.3×10^{-2} Ω·cm respectively both measured using a four-point probe (Keithley 580 Micro-Ohmmeter).

The flexibility and electrical stability of the AZO films deposited on the transparent PEN substrate were assessed through various tests. These tests included uniaxial tensile, bending and bending fatigue tests.

The Miniature Material testing machine was utilized to conduct the uniaxial fragmentation test. In this test, in situ optical microscopy was employed to capture images at intervals of 3 seconds. This enabled the monitoring of the critical onset strain and the progression of crack formation in the thin film as the applied tensile strain increased. The National Instruments LabVIEW software was employed to track changes in resistance during the test. Figure 1 illustrates the device used for this purpose.

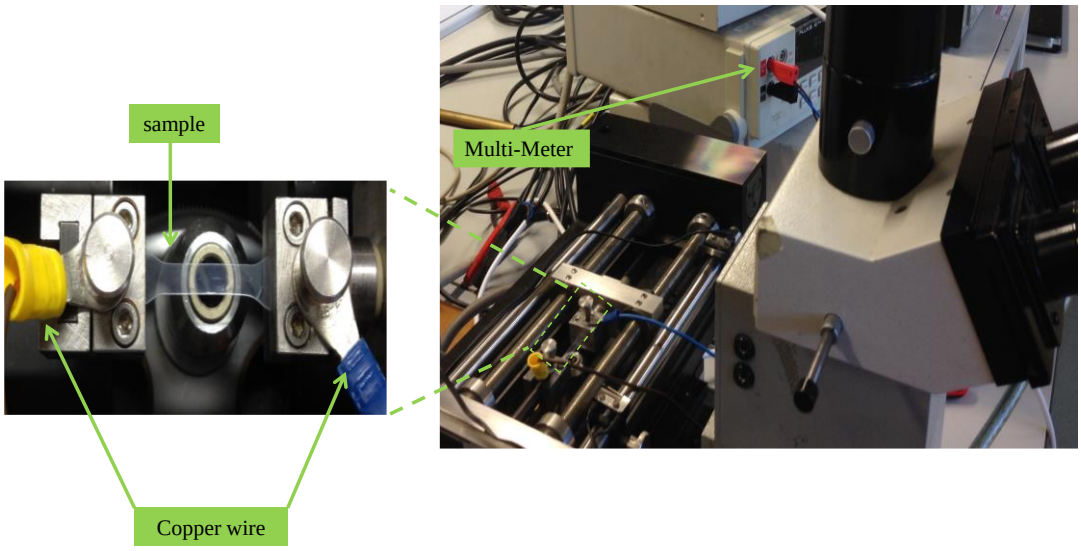

Fig. 1. Miniature Materials Tester (Minimat) with sample coupled to an optical microscope

During the experiment, the samples were subjected to a strain rate of 0.1 mm/min. It was observed that when the loading rate was too fast under continuous loading conditions, focusing the microscope became challenging. However, employing a slow loading rate of 0.1 mm/min enabled precise capture of the crack pattern.

The analysis of AZO film cracking involved examining the crack density (CD) at each increment of applied strain. The crack density, defined as the inverse of the average spacing between the cracked AZO thin film, was determined through the use of image analysis software (Image J) on optical microscope photographs.

Based on other studies [12], the bending experimental apparatus used in this study was modified. The 30×4 mm specimens were mounted between two parallel plates, one of which was movable and bent at a crosshead speed of 0.5 mm/min, while the other plate stayed in place. A confocal laser scanning microscope (CLSM) was coupled with the bending equipment Figure 2 to observe crack propagation and identify crack onset strains during both tension and compression. In this investigation, the plates were modified in order to evaluate electrical resistance. To create a closed electrical circuit, a polytetrafluoroethylene (PTFE) foil was specifically placed between one plate and the bending rig. Furthermore, the plate was fastened to the bending rig using PTFE screws. In addition, a FLUKE 45 multimeter was attached to both plates via two copper wires in order to measure the electrical resistance in situ. The sample geometry and distance between the parallel plates were quantified using a side-view digital imaging system and they were analyzed using image analysis software (Image J). The bending radius of the samples was determined according to the procedures outlined in references [13–15], and the resulting strain from bending was computed using the equation [16–18]

$$\varepsilon = \frac{h_s}{R} \tag{1}$$

where R is the radius of curvature and h_s is substrate thickness

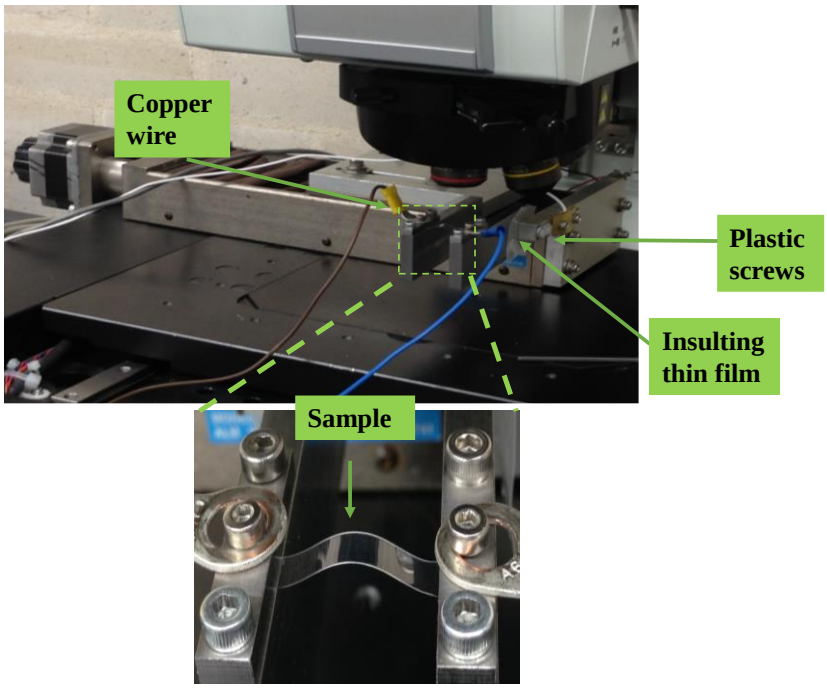

Fig. 2. Image of the bending test set-up used in this study

The bending fatigue test was conducted using an ADMET MTESTQuattro mechanical testing unit (Figure. 3). The test employed a tensile sawtooth profile with a servo-controlled displacement rate of 2 mm/min up to 1% strain. For electricity to flow, a strip of copper foil was used. In-situ monitoring of electrical resistance change was achieved using a digital multimeter Agilent 34970A.

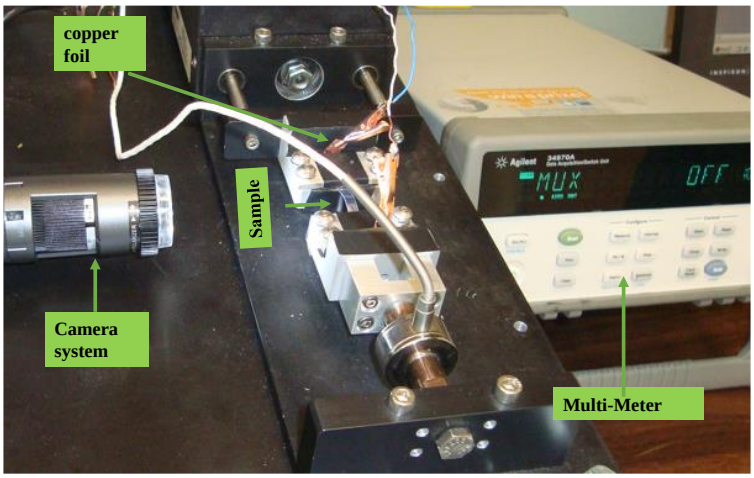

Fig. 3. The bending fatigue experiment set-up used

To analyze the cracking morphology of the AZO films after testing, scanning electron microscopy (SEM) was employed. Before conducting SEM observations, the samples were coated with a 5 nm gold layer to prevent electron charging. The images were captured using an accelerating voltage of 15 kV and a working distance of 10 mm.

RESULTS AND DISCUSSION

During the tensile testing, the AZO/PEN surface underwent uniaxial strain while in-situ monitoring electrical resistance and surface optical microscopy. The point at which cracks began to form was determined using two monitoring tools: normalized electrical resistance (COS-R) and optical microscopy (COS-M). COS-R values were derived from a sudden 10% increase in electrical resistance, COS-M refers to the strain at which the first cracks in the coating were visually observed, and this value is used to define the crack onset strain [19,20].

In Figure 4, it is observed that a typical progression of cohesive failure occurs under tensile strain. The onset of cracks happens when the externally applied strain reaches a critical value of approximately 3.1 ± 0.32% (COS-M). These cracks are believed to originate from imperfections or defects that persist in the layer after deposition, as depicted in Fig. 4(a). This observation suggests that such imperfections contribute to an increased energy release in the region. The interface separation around an imperfection leads to a larger energy release rate compared to a defect-free surface [21]. The initial crack growth measured from micrographs showed good agreement with the crack onset strain (COS) values, which corresponded to a 10% increase in normalized electrical resistance. As the applied strain level continues to increase, at approximately ~6.4% strain of AZO-coated PEN, an adhesion-related failure in the form of buckling of the AZO film appears [22].

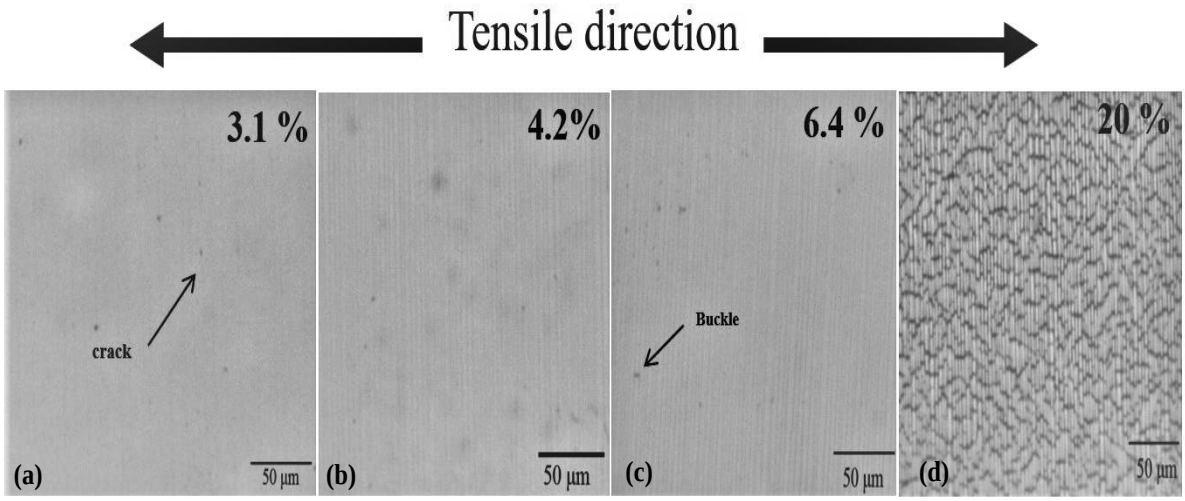

Fig. 4. Crack patterns of AZO-coated PEN substrate as nominal stresses increase. The arrows indicate the direction of elongation, and corresponding strain values are indicated on the images

Upon conducting SEM analysis, it was confirmed that cracks do exist on the top of the buckle, aligned parallel to the applied tensile strain. These secondary cracks indicate open buckling zones, as demonstrated in Figure 5. The appearance of secondary cracks and buckling of the film seemed to result from a lateral contraction of the sample, which results from Poisson [23–27] Additionally, an important observation was made that the AZO/PEN samples had cracked at the edges of the debonded zone, confirming a higher adhesion level of AZO-coated PEN systems.

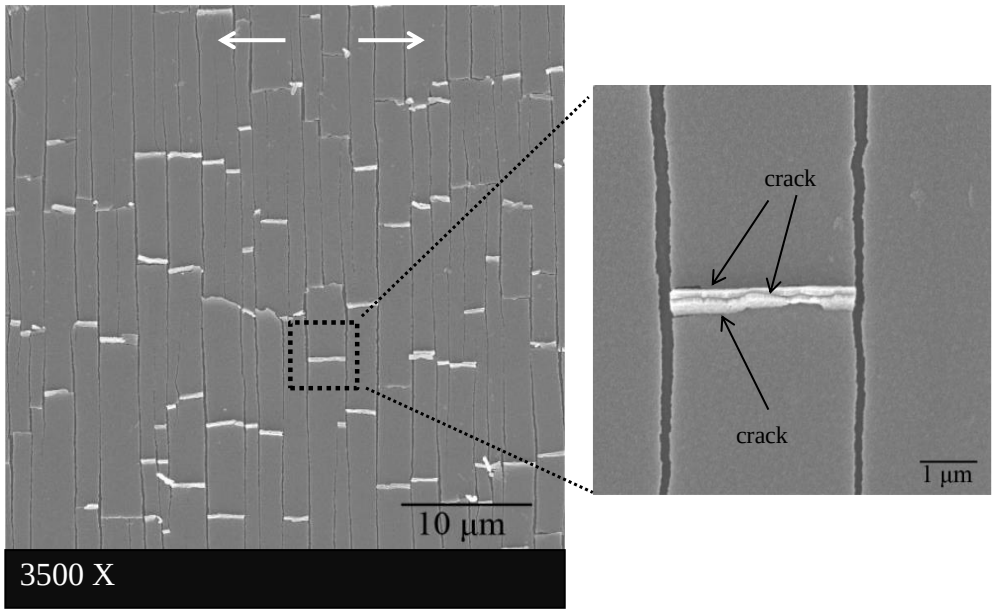

Fig. 5. FIB-SEM image of buckling delamination of 75 nm AZO film at 16% (the black arrows are indicating the locations of the initiation of crack at the edges of the debonded zone and on the top of the buckle, and the white arrow indicate the direction of the applied tensile strain)

Figure 6 illustrates the crack density and the variation in electrical resistance of the conductive layer, represented as $\Delta R/R_o$, where $\Delta R = R - R_o$. Here, R_o denotes the electrical resistance value before applying strain, and R represents the resistance value after applying uniaxial strain. The resistance of the AZO film exhibits remarkable constancy at the outset, even as strain increases (Fig. 6). These characteristic underscores the film's ability to endure mechanical deformation until it reaches a critical strain point (COS-R). It is possible to credit this behavior to the intrinsic flexibility and initial defect-free character of the film, which enables it to tolerate slight deformations without causing considerable disruption to its conductive network. At around 3.2 ± 0.21 %, the creation of microcracks begins upon reaching the COS-R, which is indicated by 10% increase in normalized electrical resistance. This disrupts the conductive pathways and causes a progressive rise in resistance. Since seen in Figure 4 via a series of optical micrographs, there is a clear association between mechanical strain and microstructural deterioration, as the density of these cracks first rises dramatically with tensile strain. Nevertheless, at 6.6 % strain, the crack density reaches a saturation threshold at about 300 mm^{-1}. Crack density saturation is highly correlated with buckling delamination of the AZO film on the PEN substrate, this results in a reduction of the tensile stress that is transferred from the compliant substrate to the AZO [28]. This instance is shown in Figure 4(c), which demonstrates that buckling of the AZO/PEN occurs at strain approaching its saturation strain state.

The film exhibits a limited resistance even after considerable cracks, indicating the existence of conductive pathways that bridge the cracks. These pathways might be caused by newly formed conductive channels within the crack gaps or by the partial separation of film fragments [29]. For AZO films to be considered for uses where electrical conductivity and mechanical flexibility are of utmost importance, the maintenance of these pathways is critical.

Up to the threshold of crack saturation, the relationship between applied strain and crack density is clearly proportional. The further complexity of the connection may be attributed to the interaction between cracks and the formation of a percolation threshold, beyond which the introduction of more cracks has a diminished impact on the resistance.

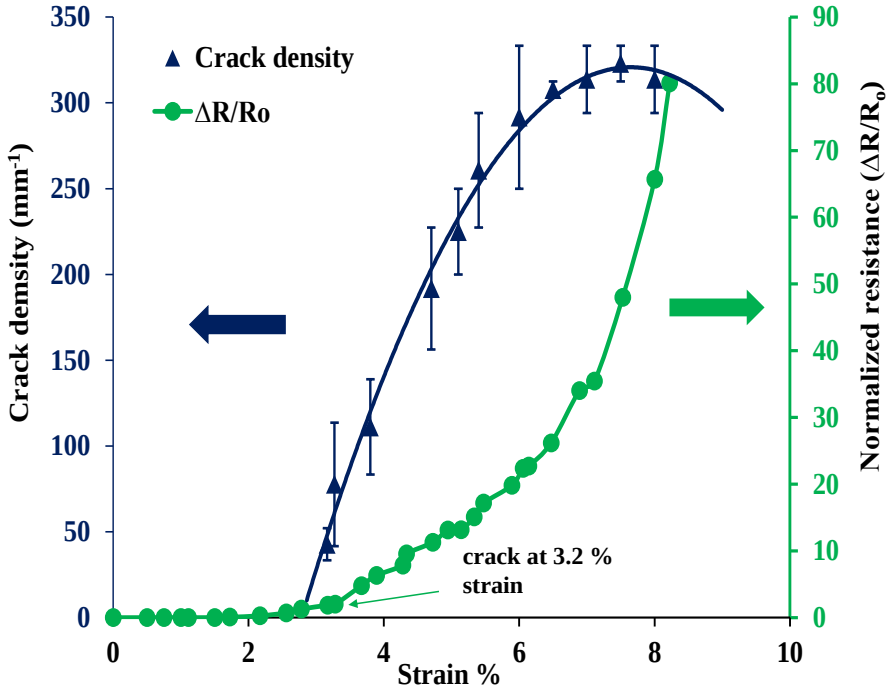

Fig. 6. Crack density and change in resistance (ΔR/Ro) of AZO (75nm)/PEN as a function of applied the strain

The initiation and development of channel cracks were examined and compared with those of ITO films studied by Sierros et al. [30] to better understand the stretchability. In comparison to the ITO film, whose change in electrical resistance started at 2.25 percent strain, The AZO film electrodes demonstrated improved stretchability.

According to Figure 7, this finding indicates that the thinner film has a stronger structural integrity, which enables it to endure more mechanical deformation before experiencing electrical deterioration. The 75 nm film shows a far slower rate of resistance rise beyond the point of crack start (COS) compared to the 200 nm film, suggesting a more gradual breakdown of conductive pathways. The phenomena may be explained by the fact that electrical characteristics deteriorate more quickly in thicker AZO films due to the higher defect density, which promotes fracture initiation and propagation. Previous studies on thin ceramic films on ductile substrates [31] have shown that the cracking threshold strain is inversely related to the square root of the film thickness, lending credence to our results. These observations not only strengthen the important relationship between film thickness and the mechanical and electrical properties of AZO films, but also emphasize the need of strict quality control and defect management during the manufacturing phase for flexible electronic applications.

The results of the bending test in both tension and compression mode are shown in Figure 8. It is demonstrated that, regardless of the deformation mode, the electrical resistance of the bent AZO films in compression mode initially decreases with decreasing bending radius. This may be because the thin film's nearby atoms and grains are closer together, which reduces the physical barriers that prevent electrons from traveling and increases mobility. However, at tension bending radius of 5.4 mm and compression bending radius of 3.9 mm, cracks and electrical resistance changes start to appear. Therefore, the critical bending radius of the AZO film was determined to be 5.4 mm for tension and 3.9 mm for compression which correspond to strains of 1.2 and 1.6 percent, respectively.

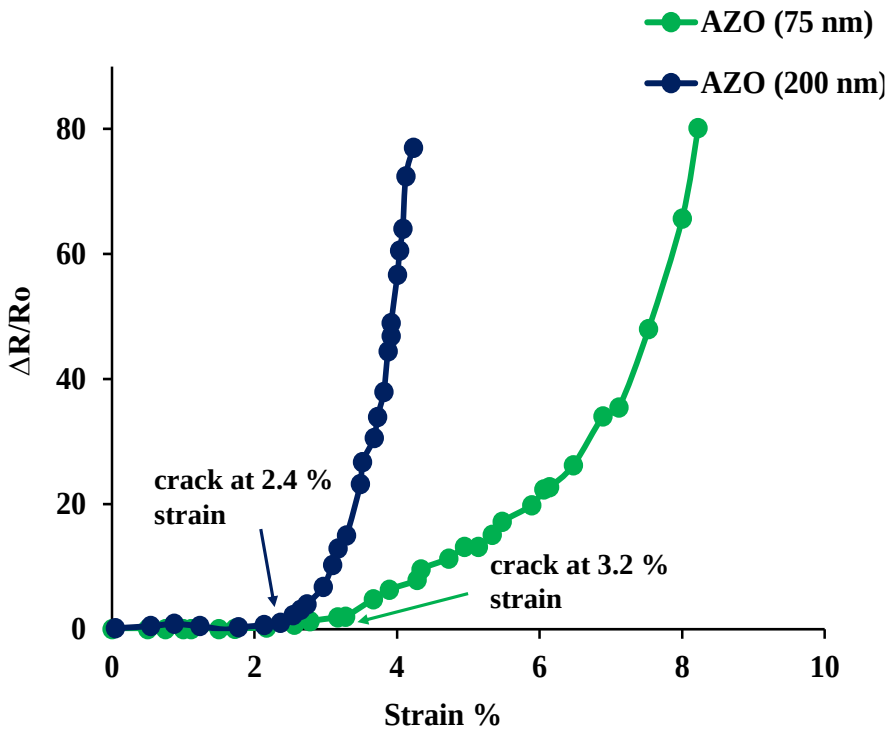

Fig. 7. Change in resistance (ΔR/Ro) as a function of the substrate nominal strain for 75 and 200 nm AZO coatings deposited on PEN substrate

These results showed that the compression bending reliability of AZO film on PEN substrates was superior to the tension bending reliability. Additionally, the number of cracks grows as the bending radius decreases, and this progressive increase in electrical resistance.

However, it should be noted that even when bending occurred below 4 mm, the ΔR/Ro value of AZO film was very small (~0.4). In contrast, reference [32], revealed that reducing the bending radius of the standard ITO electrode to 11 mm led to a significant increase in $\Delta R/R_o$. The tension and compression bending test results demonstrate that the bendability of AZO films is excellent and an ideal flexible electrode material for flexible organic solar cells.

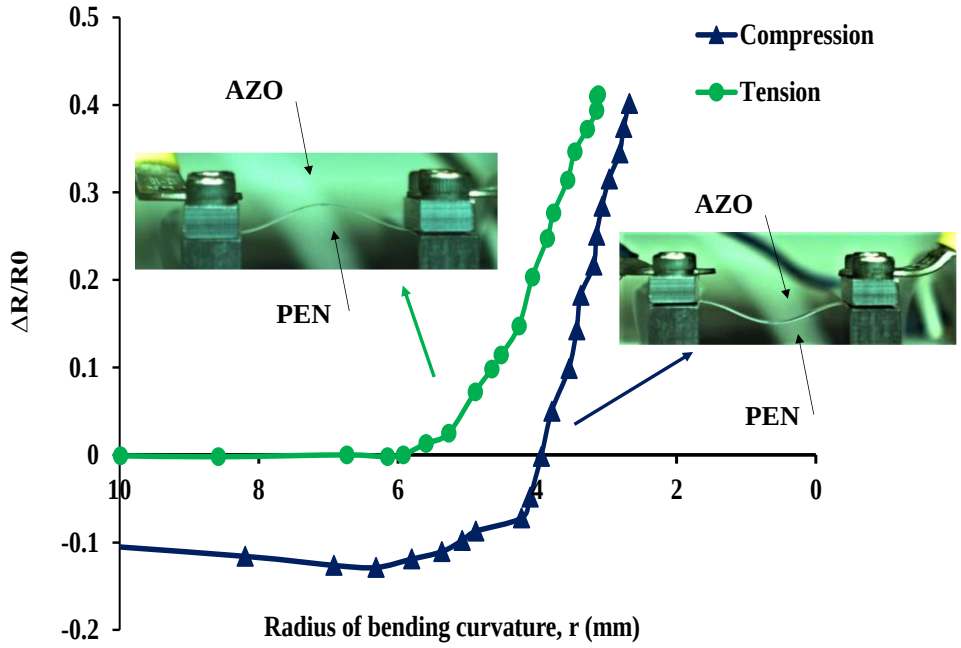

Fig. 8. Bending reliability tests in tension and compression mode with decreasing bending radius

Surface scanning electron microscopy (SEM) photographs of cracks in both AZO films after tension and compression bending tests are displayed in Figure 9. The AZO film fully split during the tension bending test seen in Figure 9(a). Figure 9(b) depicts the results of a compression bending test, in which the AZO films delaminated, fractured, and ripped off. The distinct failure mechanisms observed in the AZO film under tensile and compressive bending strains are compatible with the points of crack initiation and variations in electrical resistance.

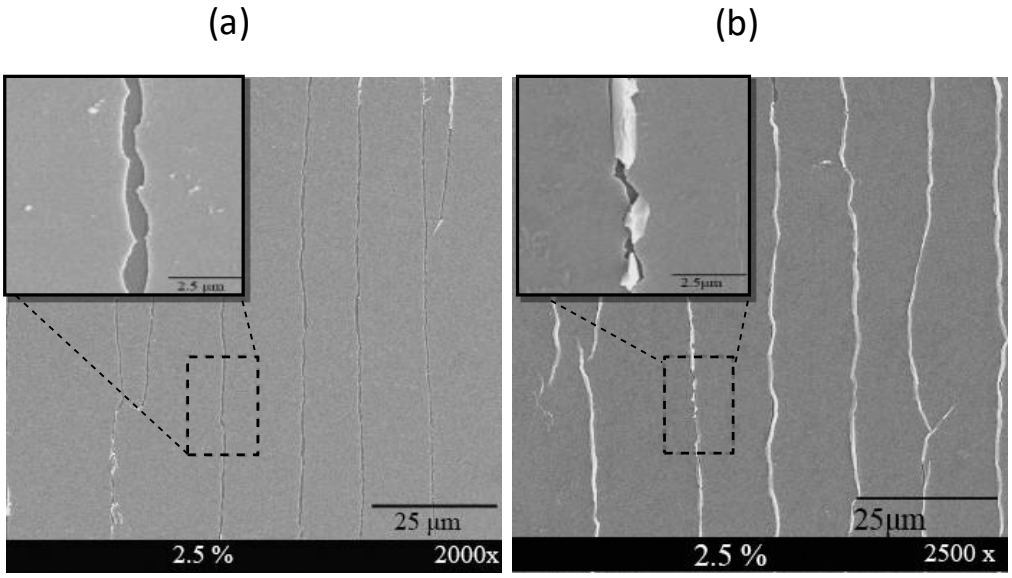

Fig. 9. SEM micrographs with enlarged images illustrating the cracking and buckling driven-delamination damage observed in a 75 nm AZO film sputtered on PEN substrates during bending test at strain 2.5 %: (a) Tensile side at strain, (b) Compression side

Figure 10 shows the tension and compression bending fatigue tests of the AZO film. Uniform AZO samples were tested at a fixed frequency of 12 s/cycle and bending radius of 6 mm which is above the critical bending radius and correspond to strain 1 %.

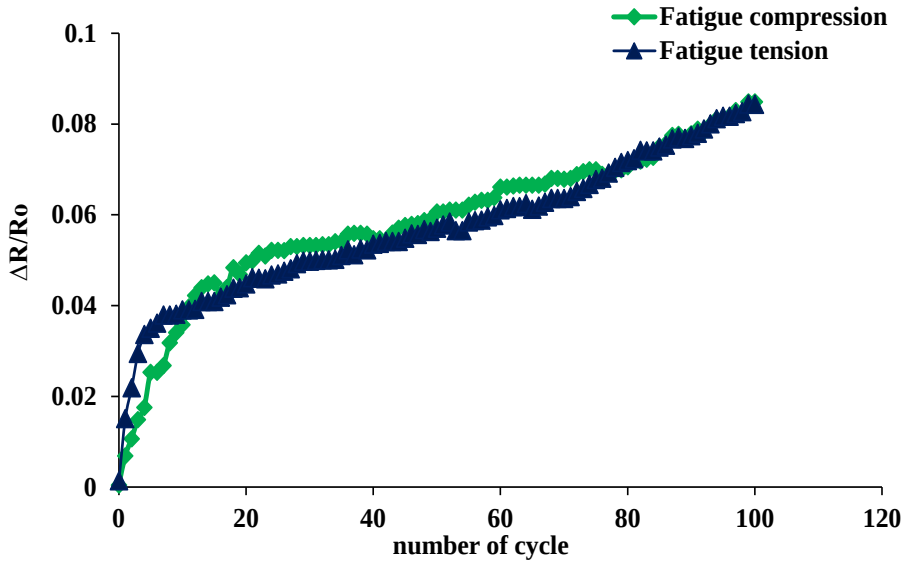

Fig. 10. Change in electrical resistance as a function of the number of cycles for AZO films deposited on PEN substrate during fatigue bending in tension and compression

The trend of the resistance change was similar, regardless of different fatigue bending conditions. The resistance abruptly increased to about 5% over the 10 cycles, and then the resistance changes become more stable and increase gradually with further increase of the number of applied bending cycles. After completion of the fatigue bending test, The AZO films in tension and compression mode showed very small increase in resistance approximately 8 %. These results indicate the AZO film's better flexibility and durability.

Since there were no visible cracks on the sample surfaces after bending fatigue testing carried out in both tension and compression modes, SEM photography has not been used in this context. However, the progressive rise in resistance seen with an increasing number of test cycles suggests that submicron cracks may exist within the AZO coating. The strain recovery that occurs during sample unloading, which causes these microcracks to close, may be responsible for the coating's lack of visible cracks.

CONCLUSIONS

The electromechanical durability of an RF–magnetron sputtered AZO film on a PEN substrate was examined using a variety of mechanical tests, including uniaxial tensile, bending, and bending fatigue tests. During uniaxial tensile tests, the crack initiation strain, the progression of crack density, and variations in electrical resistance were measured and analyzed. Crack onset strain (COS-M) ~3.1 % was shown to be associated with an abrupt rise in sample resistance. Additionally, it was shown that the thickness of the AZO coating has a significant impact on the crack initiation strain. AZO film with a thickness of 200 nm showed a low critical tensile strain of ~2.4 percent.

In the bending test in compression mode, the AZO films had great bending durability, with a critical bending radius of 3.9 mm, which is equivalent to a strain of 1.6%. Because the films overlap after a crack, there is a path for current to flow. This makes AZO films more durable under compression bending than under tension bending. Even though the AZO layer separated from the substrate, the change in electrical resistance was very small (0.4) below bending radius of 4 mm.

According to the bending fatigue test, the AZO electrode can endure 100 cycles of bending at a radius of 6 mm, regardless of the bending mode. Even after 100 cycles of loading, no cracks or delamination appeared in the AZO film, which had a very low R/R_o value of 0.08. These findings suggest that AZO film is suitable for various flexible applications and roll-to-roll manufacturing due to its substantial critical strain and small critical bending radius.

ACKNOWLEDGEMENTS

The author expresses gratitude to DuPont-Teijin for providing polymer samples. Prof. A. J. Flewitt and Dr. R. Waddingham from the Electrical Engineering Division of the Department of Engineering at the University of Cambridge are also acknowledged for providing deposition facilities. The author would like to thank Kostas Sierros for supplying the fatigue bending test apparatus at West Virginia University's Department of Mechanical & Aerospace Engineering. Dr. Steven Kukureka of the School of Metallurgy and Materials at the University of Birmingham supplied me with essential scientific help. I would also like to thank Mr. Frank Biddlestone and Mr. Warren Hay of the University of Birmingham for their technical support. Sincerely, we acknowledge financial help from the Kurdistan Regional Government's HCDP program, grant number 2DD-07.

Authors' Contribution Statement

In this research piece, I, Dilveen Waheed Mohammed would like to emphasize that I was solely responsible for the conceptualization, design, data collecting, analysis, and creation of the text. As there are no other authors linked with this article, I am completely accountable for the entirety of the material offered.

Conflict of Interest Statement

Regarding this paper, I, Dilveen Waheed Mohammed, hereby declare that there are no conflicts of interest to disclose. I conducted all of the research and effort provided in this paper; no other authors made any contributions to it.

I affirm that this research was conducted independently and that the content of this paper is the result of my own efforts, without the participation or influence of any third parties.

REFERENCES

1. H.-K. Kim, J.-W. Lim, Flexible IZO/Ag/IZO/Ag multilayer electrode grown on a polyethylene terephthalate substrate using roll-to-roll sputtering, Nanoscale Research Letters. 7 (2012) 67.
2. Q. Xu, W. Shen, Q. Huang, Y. Yang, R. Tan, K. Zhu, N. Dai, W. Song, Flexible transparent conductive films on PET substrates with an AZO/AgNW/AZO sandwich structure, Journal of Materials Chemistry C. 2 (2014) 3750.
3. X. Li, P. Li, Z. Wu, D. Luo, H.-Y. Yu, Z.-H. Lu, Review and perspective of materials for flexible solar cells, Materials Reports: Energy. 1 (2021) 100001.

4. S.-Y. Chang, Y.-C. Hsiao, Y.-C. Huang, Preparation and mechanical properties of aluminum-doped zinc oxide transparent conducting films, Surface and Coatings Technology. 202 (2008) 5416–5420.
5. C.Y. Peng, M.M. Hamasha, D. Vanhart, S. Lu, C.R. Westgate, Electrical and optical degradation studies on AZO thin films under cyclic bending conditions, IEEE Transactions on Device and Materials Reliability. 13 (2013) 236–244.
6. G.M. Wu, Y.F. Chen, H.C. Lu, Aluminum-Doped Zinc Oxide Thin Films Prepared by Sol-Gel and RF Magnetron Sputtering, 120 (2011) 149–152.
7. S. Fernández, a. Martínez-Steele, J.J. Gandía, F.B. Naranjo, Radio frequency sputter deposition of high-quality conductive and transparent ZnO:Al films on polymer substrates for thin film solar cells applications, Thin Solid Films. 517 (2009) 3152–3156..
8. K.A. Sierros, D.S. Hecht, D.A. Banerjee, N.J. Morris, L. Hu, G.C. Irvin, R.S. Lee, D.R. Cairns, Durable transparent carbon nanotube films for flexible device components, Thin Solid Films. 518 (2010) 6977–6983.
9. M.M. Hamasha, K. Alzoubi, S. Lu, Behavior of sputtered indium-tin-oxide thin film on poly-ethylene terephthalate substrate under stretching, IEEE/OSA Journal of Display Technology. 7 (2011) 426–433.
10. C.-Y. Lim, J.-K. Park, Y.-H. Kim, J.-I. Han, Mechanical and Electrical Stability Indium-Tin-Oxide Coated Polymer Substrates under Continuous Bending Stress Condition, Journal of International Council on Electrical Engineering. 2 (2012) 237–241.
11. J.L. Ni, X.F. Zhu, Z.L. Pei, J. Gong, C. Sun, G.P. Zhang, Comparative investigation of fracture behaviour of aluminium-doped ZnO films on a flexible substrate, Journal of Physics D: Applied Physics. 42 (2009) 175404(7pp).
12. C.Y. Peng, H. Sudarsanam, M.M. Hamasha, S. Lu, T.P. Dhakal, C.R. Westgate, Performance of aluminum-doped zinc oxide thin films under bending fatigue conditions, 2012 IEEE Long Island Systems, Applications and Technology Conference, LISAT 2012. (2012).
13. Z. Chen, B. Cotterell, W. Wang, E. Guenther, S. Chua, A mechanical assessment of flexible optoelectronic devices, Thin Solid Films. 394 (2001) 202–206.
14. D.W. Mohammed, R. Waddingham, A.J. Flewitt, K.A. Sierros, J. Bowen, S.N. Kukureka, Mechanical properties of amorphous indium-gallium-zinc oxide thin films on compliant substrates for flexible optoelectronic devices, Thin Solid Films. 594 (2015) 197–204.
15. D.W. Mohammed, Mechanical and electro-mechanical reliability of transparent oxide thin films for flexible electronics applications, PhD thesis, University of Birmingham, 2016. https://doi.org/https://etheses.bham.ac.uk//id/eprint/7997/1/Mohammed17PhD.pdf.
16. Z. Chen, A mechanical assessment of flexible optoelectronic devices, Thin Solid Films. 394 (2001) 201–205.
17. Q. Guan, J. Laven, P.C.P. Bouten, G. De With, Mechanical failure of brittle thin films on polymers during bending by two-point rotation, Thin Solid Films. 611 (2016) 107–116.
18. M.J. Cordill, P. Kreiml, H. Köstenbauer, C. Mitterer, A comparison of 90◦ bending for foldable electronics, Coatings. 14 (2024) 98.
19. D.W. Mohammed, R.B. Ameen, K.A. Sierros, J. Bowen, S.N. Kukureka, Twisting fatigue in multilayer films of Ag-alloy with indium tin oxide on polyethylene terephthalate for flexible electronics devices, Thin Solid Films. 645 (2018) 241–252..
20. G.A. Potoczny, Electro-Mechanical Behaviour of Indium Tin Oxide Coated Polymer Substrates for Flexible Electronics, (2012).

21. A.A. Abdallah, P.C.P. Bouten, J.M.J. den Toonder, G. De With, Buckle initiation and delamination of patterned ITO layers on a polymer substrate, Surface and Coatings Technology. 205 (2011) 3103–3111.

22. Z. Zhao, H. Fu, R. Tang, B. Zhang, Y. Chen, J. Jiang, Failure mechanisms in flexible electronics, International Journal of Smart and Nano Materials. 14 (2023) 510–565.

23. T.S. Bejitual, D. Compton, K.A. Sierros, D.R. Cairns, S.N. Kukureka, Electromechanical reliability of flexible transparent electrodes during and after exposure to acrylic acid, Thin Solid Films. 528 (2013) 229–236.

24. S. Frank, U. a. Handge, S. Olliges, R. Spolenak, The relationship between thin film fragmentation and buckle formation: Synchrotron-based in situ studies and two-dimensional stress analysis, Acta Materialia. 57 (2009) 1442–1453.

25. L. Rebouta, L. Rubio Pena, C. Oliveira, S. Lanceros-Mendez, C.J. Tavares, E. Alves, Strain dependence electrical resistance and cohesive strength of ITO thin films deposited on electroactive polymer, Thin Solid Films. 518 (2010) 4525–4528.

26. M. J. Cordill, Kreiml, P., C. Mitterer, Materials Engineering for Flexible Metallic Thin Film Applications, Materials. 15 (2022) 1–25.

27. J. Zhou, X. Zhang, X. Zhang, W. Zhang, J. Li, Y. Chen, H. Liu, Y. Yan, Mechanical Properties of Tensile Cracking in Indium Tin Oxide Films on Polycarbonate Substrates, Coatings. 12 (2022) 1–12.

28. D. Tsubone, T. Hasebe, A. Kamijo, A. Hotta, Fracture mechanics of diamond-like carbon (DLC) films coated on flexible polymer substrates, Surface and Coatings Technology. 201 (2007) 6423–6430.

29. D.R. Cairns, R.P. Witte, D.K. Sparacin, S.M. Sachsman, D.C. Paine, G.P. Crawford, R.R. Newton, Strain-dependent electrical resistance of tin-doped indium oxide on polymer substrates, Applied Physics Letters. 76 (2000) 1425.

30. K. Sierros, N.J. Morris, S.N. Kukureka, D.R. Cairns, Dry and wet sliding wear of ITO-coated PET components used in flexible optoelectronic applications, Wear. 267 (2009) 625–631.

31. J.I. Han, Stability of Externally Deformed ITO Films, in: G.P. Crawford (Ed.), Flexible Flat Panel Displays, John Wiley & Sons Ltd, Chichester, 2005: pp. 121–132.

32. Y. Zhi-nong, X. Fan, L. Yu-qiong, X. Wei, The electrical stabilities of flexible ITO thin films on buffer layer coated PET, Optics Info Base Conference Papers. (2008) 3–5.